WIND ENERGY SCIENCE DISCUSSIONS

Open Access

european academy of wind energy

Interactive comment on "Does the wind turbine wake follow the topography? – A multi-lidar study in complex terrain" *by* Robert Menke et al.

Robert Menke et al.

rmen@dtu.dk

Received and published: 5 July 2018

Response to reviewer 1 (Michele Guala)

We thank Michele Guala for his critical feedback which helped us to improve this manuscript. Below we answer his specific comments in detail:

Comment 1

I have some reservation on the atmospheric stability assessment: |z/L| <0.01 is a very strict condition for the neutral regime, rarely observed from micrometeorological data from sonic anemometers. Based on Fig 6 it seems that it occurs quite frequently. I am wondering how accurate is the estimate of the turbulent heat flux and how far from the

surface (the actual z) is the estimate referring to.

The |z/L| used in the stability assessment is derived from the RMOL variable in the WRF output, which is from the formulation in the MYNN2 PBL and surface layer scheme (Nakanishi and Niino 2006) and is computed at the model surface (10m). As mentioned in the manuscript, there is some evidence that the WRF model has shown good skill at simulating their climatology (see e.g. Fig 6 in Draxl et al, 2014). The limit of |z/L| < 0.01 is also used by Muñoz-Esparza et al. (2012) who suggests a limit of |L| > 1000.

Comment 2

More importantly the Monin Obukhov similarity assumes a logarithmic region where the mean velocity profile is distorted by the thermal stability effect. In complex terrain the contributions to mechanical production of turbulent kinetic energy may be more complicated as compared to the $u_\star^3/kz$ term that is likely employed here. The authors should provide the definition of L and discuss how they account for the non-flat topography and for the orientation of the reference system with respect to the mean incoming wind (likely non flat and to some extent following the terrain).

We are aware that the Monin Obukhov theory is meaningless when calculated for flow over complex terrain from mast measurements. However, the simulation results of the WRF model employed in this study are based on a 3 km x 3 km grid of the smallest domain. Terrain features which are small compared to the model resolution, like the Perdigão ridges, are thus not visible to the model and are only represented by an increased surface roughness. The model sees only a smoothed surface which makes it possible to derive the Obukhov length from the simulation. Confidence in the results is gained by a comparison of the WRF results with the diurnal cycle (Figure 1). The distribution shows a clear separation of the results in a day and night time regime. This distribution corresponds well with observations made by us in the field during the campaign. The period of the campaign was generally very hot and dry with maximum

temperatures above 40°C.

Comment 3

Fig 7: the wake deficit depends on the turbine operating conditions: it would be relevant to provide the tip speed ratio and the power coefficient for the wake plotted in Fig 7b (at least the 10min corresponding averaged value).

We added the tip speed ratio and power coefficient based on the 10 minute averages from the SCADA system of the turbine to the manuscript.

Comment4

Despite of many hours of measurements, the most interesting figures show results from quasi-instantaneous measurements. I wonder if it is possible to use conditional averages or two point correlation to support the conclusion with statistics instead of single realization. Perhaps, the wind tunnel work by KB Howard, LP Chamorro, and M Guala "comparative analysis on the response of a wind-turbine model to atmospheric and terrain effects" Boundary-layer meteorology 158 (2), 229-255, 2015 may offer some ideas

We will consider employing the two-point correlation technique for further work that will be done also in combination with a new dataset that was measured during the Perdigão 2017 campaign at the same measurement site.

Comment 5

Fig 10b: how is the wake deflection angle estimated? within a range of x/D? based on the velocity contour, a velocity minima envelope? Please clarify

The length of the wake in the Diamond scan is estimated by the velocity contour. This information has been added to the manuscript.

Comment 6

For non LiDAR experts, perhaps the definition of radial velocity should be provided. Some of the velocity contour distribution with height presented in fig 9b are prone to be misinterpreted without a proper definition.

The definition of radial velocity has been included in the manuscript and the description of the RHI scanning trajectory has been advanced.

References

Draxl, C., Hahmann, A. N., Peña, A. and Giebel, G.: Evaluating winds and vertical wind shear from Weather Research and Forecasting model forecasts using seven planetary boundary layer schemes: Evaluation of wind shear in the WRF model, Wind Energy, 17(1), 39–55, doi:10.1002/we.1555, 2014.

Muñoz-Esparza, D., Cañadillas, B., Neumann, T. and van Beeck, J.: Turbulent fluxes, stability and shear in the offshore environment: Mesoscale modelling and field observations at FINO1, Journal of Renewable and Sustainable Energy, 4(6), 063136, doi:10.1063/1.4769201, 2012.

Interactive comment on Wind Energ. Sci. Discuss., https://doi.org/10.5194/wes-2018-21, 2018.

Fig. 1. Diurnal cycle of the Obukhov length for the period of the measurement campaign.

C5

WIND ENERGY SCIENCE DISCUSSIONS

eawe
european academy of wind energy

Open Access

Interactive comment on "Does the wind turbine wake follow the topography? – A multi-lidar study in complex terrain" *by* Robert Menke et al.

Robert Menke et al.

rmen@dtu.dk

Received and published: 5 July 2018

Response to reviewer 2

We thank the anonymous reviewer for her or his feedback and comments. Below we answer the specific comments in detail:

Comment 1
Since the scan strategy is not suited to study more than a couple of rotor diameters of the wake extent, it would be useful to go into the details of the deficit magnitude. For example, does the deficit magnitude vary as a function of turbine operation and stability?

Printer-friendly version

Discussion paper

It would be interesting to analyze the relation of wake deficit to other parameters. However, we cannot determine where exactly the scanning trajectory (Diamond Scan) cuts the wake makes it impossible to determine the absolute velocity deficit. This fact prohibits to set the deficits derived from the Diamond scan in relation to the atmospheric stability or turbine operational parameters. We are addressing this issue in section 4.1: "Such a misalignment causes that deficits profiles measured with the Diamond scan are not necessarily located in the wake center. Nevertheless, in short distance to the turbine, the wake misalignment with the Diamond Scan is expected to be small, which allowed calculating an average deficit for specific sectors in a distance of one rotor diameter. Consequently only selected periods can be investigated over the entire length of the Diamond Scan."

Comment 2

From Figure 9, I see that the deficit minimum at the wake center seems to exhibit different characteristics for the four different cases. For example, the length of the minimum at the center seems to vary for the different conditions. Is this a function of the stability or turbine operation? Do these differences show up in the other cases?

The operational state of the turbine and atmospheric conditions have undoubtedly an influence on the wake characteristics. The wake measurements shown in figure 9 are used to illustrate the strong vertical wake displacements. Differences in the wake characteristic observed with the Diamond Scan are a combination of different angles between wake and scanning plane, atmospheric conditions and the operational state of the turbine. Unfortunately, it is not possible with the available measurements to isolate one of these factors.

Comment 3

There are a few places in the manuscript that could use some grammar corrections. I have identified some of them. However, I am not proficient in English myself and

therefore it might be a good idea to get this manuscript proof read by an expert rather than rely on my suggestions.
1) Page 1, line 14: "cause" and not "are causing"
2) Page 1, line 20: "cover" and not "are covering"
3) Page 5, line 7: "cause" and not "are causing"

Thanks for these corrections. We carefully read the manuscript again to improve the presentation of this research.

Interactive comment on Wind Energ. Sci. Discuss., https://doi.org/10.5194/wes-2018-21, 2018.

Does the wind turbine wake follow the topography? - A multi-lidar study in complex terrain

Robert Menke[1], Nikola Vasiljević[1], Kurt S. Hansen[2], Andrea N. Hahmann[1], and Jakob Mann[1]

[1]Technical University of Denmark - DTU Wind Energy, Fredriksborgvej 399, Building 118, 4000 Roskilde, Denmark
[2]Technical University of Denmark - DTU Wind Energy, Nils Koppels Allé, Building 403, 2800 Kgs. Lyngby, Denmark

Correspondence to: Robert Menke (rmen@dtu.dk)

Abstract. The ~~wind turbine~~ wake of a single wind turbine in complex terrain is analysed using measurements from lidars. A particular focus of this analysis is the wake deficit and propagation. Six scanning lidars, three short-range and three long-range WindScanners, were deployed during the *Perdigão 2015* measurement campaign, which took place at a double-ridge site in Portugal. Several scanning scenarios, including triple- and dual- Doppler scans, were designed to capture the wind turbine wake of a 2 MW turbine located on one of the ridges. Different wake displacements are categorised according to the ~~diurnal cycle~~ time of the day. The results show a strong dependence of the vertical wake propagation ~~to~~ on the atmospheric stability. When a ~~terrain- induced~~ terrain-induced gravity wave is observed under stable conditions, the wake follows the terrain down the ridge with a maximum inclination of -28°. During unstable conditions, the wake is advected upwards by up to 29° above ~~horizontal~~ the horizontal plane.

1 Introduction

Detailed knowledge about the behaviour of wind turbine wakes is essential for the design and the operation of wind farms. The wake is a region of reduced wind speed and increased turbulence in the downwind direction behind a wind turbine. It is caused by the extraction of kinetic energy from the wind field. As the wake propagates, it can affect other turbines in the downwind direction~~. Turbines in the wake region~~, which will produce less power due to the reduced kinetic energy of the flow (Barthelmie et al., 2007). Additionally, higher turbulence levels in the wake ~~are causing~~ cause high fatigue loads, which in turn reduce the lifetime of wind turbines (Bustamante et al., 2015; Thomsen and Sørensen, 1999). Due to these facts and the trend to erect turbines in wind farms where turbines are relatively closely packed together, a detailed understanding of the wake propagation is imperative. Frequently applied computer models in the wind farm planning process ~~are including~~ include simplifications that are acceptable for sites with simple a orography. For example, the linearised model WAsP ~~assume~~ assumes that the wake follows the shape of the terrain in the downstream direction (Troen and Petersen, 1989). More sophisticated approaches like computational fluid dynamics (CFD) models and large eddy simulations (LES), do not constrain the wake propagation but ~~are covering~~ cover prevailingly neutral atmospheric conditions apart from few academic studies (e.g. convective instabilities: Mirocha et al. (2014); stable conditions: Aitken et al. (2014); Bhaganagar and Debnath (2015); both convective and stable: Mirocha et al. (2015); Vollmer et al. (2016); Abkar and Porté-Agel (2015); Englberger and Dörnbrack (2017). ~~In order to~~

To investigate to which degree these assumptions and limitations are applicable to real flow cases, we performed a full-scale experiment in complex terrain using wind lidars.

Wind lidars are available as continuous wave (CW) or pulsed systems. CW lidars are capable of providing high-frequency measurements of the line-of-sight (LOS) speed (up to 400 Hz, Vasiljević et al., 2017). However, at any given measurement rate CW lidars can only measure the LOS speed from a single range. Since the range determination is achieved by focusing the laser beam at a given point, the probe length is not constant with range. In fact, the probe length increases with the square of the range (Mikkelsen et al., 2008). This limits the maximum range of current CW lidars to about 150 m. Nevertheless, their capability of observing the wind field with a high frequency and relatively small probe lengths makes them ideal for studies of both mean and turbulent properties of the near wake in a region of up to two rotor diameters such as performed by Bingöl et al. (2010) and Trujillo et al. (2011). Unlike CW lidars, pulsed lidars can simultaneously measure LOS wind speeds from a number of ranges e.g., several hundred ranges in case of long-range WindScanner (Vasiljević et al., 2016), while their probe length is constant. The typical probe length is 30 m. Depending on their design, pulsed lidars can achieve a measurement range of up to 12 km (Krishnamurthy et al., 2013). However, pulsed lidars have a lower measurement rate than CW lidars, ~~of~~ typically around 1 Hz. Due to the aforementioned characteristics, pulsed lidars are suitable for observations of the mean properties of the flow over larger distances and are used to study the far wake of wind turbines ~~such as performed by Käsler et al. (2010) and Iungo and Porté-Agel (2013)~~(i.e. Käsler et al., 2010; Iungo and Porté-Agel, 2013).

To the knowledge of the authors, the wake behaviour in highly complex terrain has not been investigated. All existing investigations of wakes with lidars took place in flat or moderately complex terrain and offshore (Bingöl et al., 2008; Rhodes and Lundquist, 2013; Smalikho et al., 2013; Aitken and Lundquist, 2014; Vollmer et al., 2015; Machefaux et al., 2016; Herges et al., 2017; Bodini et al., 2017). The present study focuses on wake measurements of a turbine located in highly complex terrain. During the *Perdigão 2015* campaign which was a precursor for the larger *Perdigão 2017* campaign (Witze, 2017), the wake of a single wind turbine located on one of two parallel ridges was ~~measured~~scanned. The terrain is characterised by patchy vegetation and an steep orography. For this purpose, six scanning lidars were deployed during a field campaign in the late spring and early summer of 2015, which is a part of a series of atmospheric experiments for wind energy (Mann et al., 2017). Three of the six lidars are long-range WindScanners (LRWS), pulsed Doppler lidars (Vasiljevic, 2014; Vasiljević et al., 2016) and three are short-range WindScanner (SRWS), CW wave lidars (Mikkelsen et al., 2008). The WindScanner system allows ~~to measure~~ for the measurement of synchronised trajectories, thereby the retrieval of all three wind components is possible. The combination of both systems allows measuring the near and far wake, which is a novelty for wake measurements. The measurement analysis is concentrated on the vertical wake propagation and its relation to atmospheric stability. This dependency is of particular interest for turbines located in complex terrain in regions that are subjected to strong radiative forcings, ~~for example,~~ e.g. the Mediterranean region. In these regions, the atmosphere is normally stable during the night and unstable during the day.

The paper is organised as follows. An overview of the designed scanning trajectories and a general description of the campaign is presented in section 2. In section 3 the available data and methods of ~~the~~ their processing are introduced. Moreover,
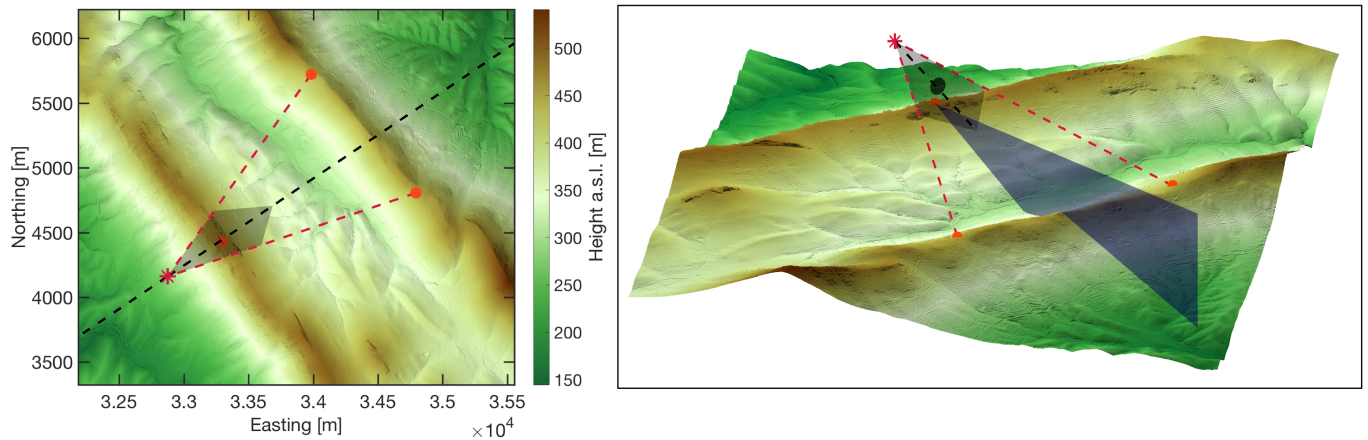
Figure 1. Overview of the terrain and scanning trajectories. Coordinates expressed in datum ETRS89/PTM06 and height above sea level. (red points: location of long-range WindScanners, blue plane: RHI scan, black circle: rotor plane, black plane: Diamond Scan plane, black dashed line: wind turbine transect or line of synchronised measurements in Diamond Scan, red dashed line: example of beams doing a measurement). Left: top view, Right: tilted view.

a new method to determine the inflow velocity in complex terrain is presented. Section 4 presents the results of the wake deficit analysis and wake propagation investigation. A summary and the conclusions of this work are given in the last section.

2   Field campaign overview

The *Perdigão 2015* field campaign took place during the months of May and June in 2015. The site was selected to meet several
5   scientific objectives. A detailed overview of the entire campaign is presented in Vasiljević et al. (2017). In this section, we ~~will~~
give a summary of the campaign and site characteristics relevant for the measurements of the wind turbine wake.

2.1   Measurement site

The main characteristic of the site are two ridges that run in parallel for a distance of 2 km (Figure 1 and 2). The ridge to ridge distance is about 1.4 km and the valley bottom to ridge peak height equals to about 200 m. The ridges run from the
10   southeast towards the northwest. ~~To the northeast and southwest, the~~ The orography is generally lower to the northeast and southwest. The roughness of the terrain is determined by rocks and ~~a~~ patchy vegetation of pine and eucalyptus trees. A former three-year assessment of the wind conditions by a 40 m tall meteorological mast ~~,~~ located on the southwest ridge about 1 km in the south west of the wind turbine ~~, over three years~~ shows two prevailing wind directions, northeast and southwest. These wind directions are perpendicular to the ridges. The wake measurements are obtained for a single Enercon E-82 2MW wind
15   turbine located on the southwest ridge (see figure 2). This turbine has a hub height of 78 m and a rotor diameter of 82 m. It is designed as a low-wind speed turbine with a cut-in wind speed of 2 m/s. The terrain around the turbine drops of several tens of
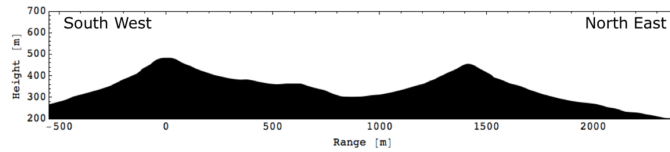
Figure 2. Wind turbine transect oriented 54° to North. The wind turbine is located at 0 m range.

meters towards the southwest. Towards the northeast, the terrain slants down towards the valley after a smaller escarpment of about 20 meters height.

2.2 WindScanner measurements

Two WindScanner systems were deployed in the *Perdigão 2015* campaign, a short-range and a long-range WindScanner sys-
5 tems consisting of three short-range lidars and long-rage lidars, respectively. The short-range system was positioned close to the turbine, considering the shorter range and the probe volume size. For the SRWS the probe length increase quadratically with the measurement distance from about 0.2 m at 10 m to 40 m at 150 m. Consequently, to keep the spatial averaging small, a measurement scenario is designed to measure the near wake of the turbine. The scenario consists of a vertical plane, perpendicular the turbine transect in the northeast of the wind turbine. Horizontally, the plane is centred at the
10 turbine location extending 48 m to each side~~, vertically~~. Vertically, the plane extends from 30 m above the height of the turbine foundation to 128 m. The three SRWSs acquired synchronised measurements in this plane along 16 vertical lines ~~(compare figure 9b in Vasiljević et al., 2017)~~(compare Figure 9b in Vasiljević et al., 2017). Accordingly, all three wind components (u, v, w) were measured. The 312 points were scanned 9 times during a 10-minute period, the system was started manually according to the present wind direction.
15 For the LRWSs, i.e. the pulsed lidars, the pulse length is the defining factor of the probe length. Considering relatively short distances of the test site a 200 ns pulse ~~has been~~ was selected. With that pulse, the full-width half maximum of probe length is 35 m and the maximum measurement distance to about 3 km. For two scanners positioned on the Northeast ridge (Figure 1) a measurement trajectory ~~has been~~ was designed to measure both the turbine inflow and its wake in an almost horizontal plane. The plane is defined by the position of the two scanners and the wind turbine nacelle, resulting in an inclination of 4.7°. The
20 scanners were configured to acquire synchronised measurements in this plane along a line orientated 54° towards north with its centre at the wind turbine's nacelle. Due to the synchronous intersection of the two laser beams along ~~the~~ this centre line instantaneous quasi-horizontal wind speeds and directions can be resolved. Measurement points are placed every 20 m, thus 50 in total, together with 2450 additional range gates placed next to this line, resulting in a diamond shaped plane with the dimensions of 500 m × 750 m. The scanners measured this trajectory, named Diamond Scan, every half an hour for 10 minutes.
25 A single scan took 25 s, resulting in 24 scans per 10-minute period. An RHI scan, a scan with constant azimuth angle and changing elevation angle, toward the Northeast along the wind turbine transect (Figure 1), was carried out by the third LRWS positioned close to the wind turbine. The scan covered elevation angles from −12.5° to 20.5°. In the plane of the RHI scan, a

4

total of 12000 ~~radial~~ LOS velocities were acquired along 50 LOSs. Accordingly, this scan provides a field of LOS velocities. The LOS velocity is the flow component orientated along the lidar's laser beam. During certain periods that are analysed in detail in section 4.2, the wake could be captured with this scan and thus ~~supplementing~~ supplements the Diamond Scan in the vertical direction.

3 Data and Methods

3.1 Determination of inflow conditions

For analysing the wind turbine wake, detailed information about the inflow to the turbine is a requirement. This raises the question ~~on~~ of how the inflow conditions can be described in complex terrain and particularly in this study. The IEC standard (IEC, 2005) provides that a reference measurement should be taken at a position 2 – 4 rotor diameters upwind from the turbine. Such an approach is not appropriate in complex terrain. Influences of the orography, like the escarpments close to the turbine at the Perdigão site, ~~are causing~~ cause significant perturbations to the flow field over small spatial scales.

Accordingly, inflow measurements should be taken close to the turbine, but at positions where the influence of the wind turbine itself to flow field is insignificant. To describe the turbines influence to the flow field, a model presented by Conway (1995) is chosen. The model shows analytically the influence of the rotor to the flow field under a specific loading of the turbine. Figure 3 shows the influence of the turbine in Perdigão on the free stream velocity (U_∞) under maximum thrust. The maximal thrust is determined from the turbine's thrust curve and is observed below rated wind speed. ~~Where~~ We difine R ~~is~~ as the radius of the wind turbine, r the radial distance from the symmetry axis of the rotor and x the distance perpendicular to the rotor. According to this model, measurement sections next to the rotor disk in the Diamond Scan are selected to represent the inflow conditions to the turbine (compare two grey sections in ~~figure~~ Figure 7a). The wind speed is averaged over two line segments, each 40 m long and positioned with a distance of 60 m to left and right of the wind turbine nacelle. The segments are always aligned perpendicular to the ~~10-min~~ 10-minute averaged wind direction calculated over the whole Diamond Scan plane. Therefore, the position of these segments changes with the wind direction. In terms of the model by Conway these segments are located in a range $r/R = 1.5$ to $r/R = 2.5$ and are at $x/R = 0$ and thus related to maximal wind speed changes ranging from 0.5% to 2.5%. However, since the blocking effect of the turbine at the position of the rotor is zero ($u/U_\infty = 1$), no effect on the selected segments is expected. For the case that the segments are not perfectly aligned with the rotor plane, the model shows that speed-up and slow-down effect cancel out in the case that the measurement volume is symmetric around the rotor, as it is in our case.

To validate this method the correlation with the wind turbine supervisory control and data acquisition (SCADA) data is investigated. The SCADA data is available as 10-minute averages for the period of the measurement campaign and includes the active power production, the nacelle direction and wind speed measured by the nacelle anemometer.From the measured
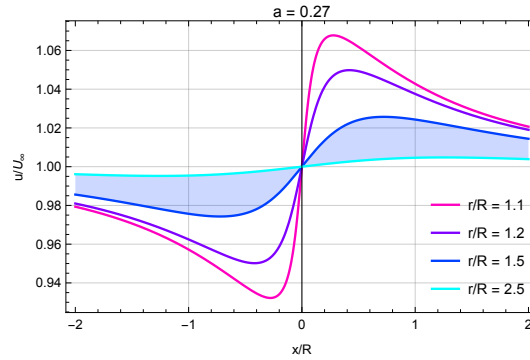
Figure 3. Solution of the actuator disk model by Conway (1995) for a induction factor of $a = 0.27$ and different ratios of the distance to the center line r divided by the radius of the disk R. The shaded sector indicates the range in which the inflow measurement volume is located.

power production in combination with the turbine's power curve the rotor-equivalent wind speed v_{rotor} ~~(Wagner et al., 2011)~~ is derived which represents the wind speed averaged over the entire rotor disk.

$$v_{\text{rotor}R} = v_{\text{power curve}PC}(P) \tag{1}$$

where $v_{\text{power curve}}$ v_{PC} is interpolated from 1 m/s binned values of the turbine's power curve. The power curve ~~has been~~ is corrected for the Perdigão site following the IEC 61400-12 standard (IEC, 2005). An air density of $1.12\,\text{kg/m}^3$ is assumed resulting from an altitude of 562 m above mean sea level and an estimated average air temperature of ~~20~~20C°. This method is only valid up to 12 m/s~~wind speed~~, the rated wind speed of the turbine, since the power production is constant for higher wind speeds.

The linear correlation of ~~v_{rotor}~~ v_R and the wind speed acquired with the WindScanner system shows a good agreement in terms of a high coefficient of determination, $R^2 = 0.96$, and a slope close to one (figure 4). From the wind speed and direction measured by the Diamond Scan, a frequency distribution is calculated (figure 5). The rose shows the prevailing wind direction west-southwest and northeast, similar to a long-term assessment of the wind conditions at the site Vasiljević et al. (2017).

3.2 Data selection

During the campaign~~in total~~, 663 h of measurement data ~~was~~ were collected by the WindScanner systems, 110 h with the SRWS system, which was in operation from May 8 until June 3 and 553 h with the LRWS which was in operation from May 19 until June 26. These numbers reduce by applying different filtering methods, as explained in Vasiljević et al. (2017). By considering the frequency distribution (figure 5) 10 h of LRWS measurement data is available in the northeastern sector. During these periods data from both the Diamond Scan and the RHI scan is available. ~~Additional~~ Additionally, 5 h of wake measurements are available from the SRWS system. Due to technical problems, no simultaneous measurements of the wake with the two WindScanner systems ~~are~~ were collected (Vasiljević et al., 2017).
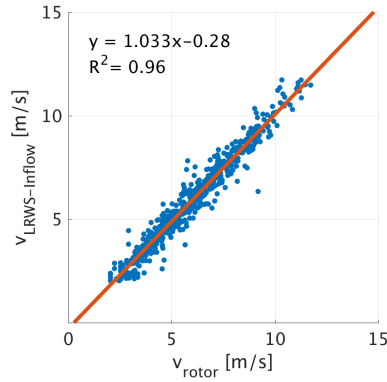
6

Figure 4. Correlation of the wind speeds derived from the Diamond Scan to the rotor equivalent wind speeds. The correlation is derived by 589 10-minute periods.
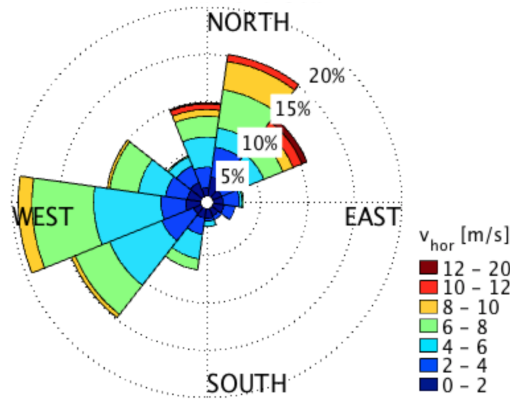

Figure 5. Sector wise frequency and velocity distribution derived from Diamond Scan measurements.

3.3 Mesoscale flow simulations

During the period of the campaign, strong radiative forcing was observed ~~which~~ that caused significant diurnal changes of the air temperature at ground level. Due to the absence of meteorological stability measurements at the site, simulations with the Weather Research and Forecasting (WRF) model are used to estimate the stability for the period of the campaign. The results are available covering the period between 1 May and 30 June 2015 and were produced with the WRF model version 3.6. For a description of the general WRF model, please refer to Skamarock et al. (2008).

The WRF model simulations were driven using ERA-Interim reanalysis datasets (Dee et al., 2011) using the method described in Hahmann et al. (2015) with the MYNN boundary layer parameterization. A total of three domains were used to downscale the flow field through one-way nesting, covering horizontal grid resolutions from 27 km to 3 km using a 1/3 ratio rule. Time series were extracted from the simulation results at the location of the wind turbine. Thermal stability was inferred
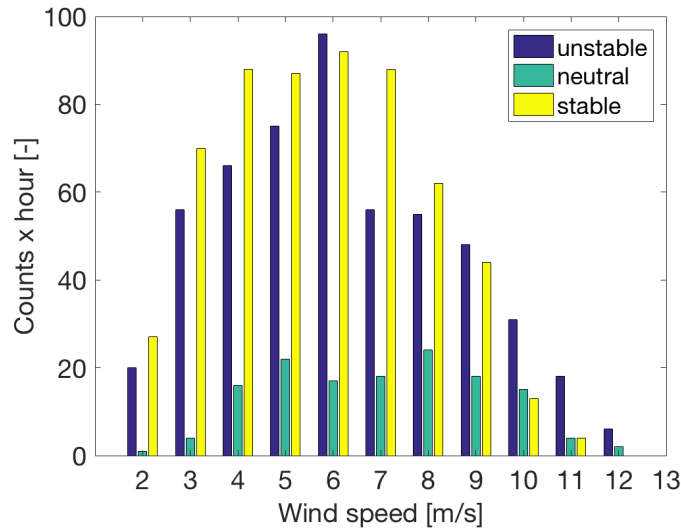
7

Figure 6. Stratification <u>of the</u> observations during the month May and June ~~.~~<u>2015.</u> The wind speed is estimated from the rotor equivalent wind speed.

from the Obukhov length L_{mo} computed at the finer 3 km domain. At the few sites where stability measurements are available, the WRF model has shown good skill at simulating their climatology (Peña and Hahmann, 2012).

The inner domain employed a $244{\times}244{\times}61$ grid with the highest vertical level set at 50 hPa. The orography was generated using ~~CORINE land surface~~ <u>USGS 30" elevation</u> data resampled according to grid resolution. Land-use categories for all domains were based on the CORINE Land Cover 2006 survey (CLC, 2006). For a detailed description of the simulation setup, please refer to Hahmann et al. (2017).

3.4 Atmospheric stratification at the wind turbine location

The WRF results show prevailingly stable atmospheric conditions during the night and unstable conditions during the day. Neutral conditions are present during transitions. We derived the stability from the Obukhov length using the following classification: stable $1/L_{mo} > 0.01$, neutral $0.01 > 1/L_{mo} > -0.01$, unstable $1/L_{mo} <$ ~~0.01~~ <u>-0.01 similar to (Hansen, 2015)</u>. The distribution of different stabilities over the calculated rotor equivalent wind speed shows that both stable and unstable stratification are well represented, while the neutral stratification is infrequently represented (figure 6).

4 Results

4.1 Wake deficit and wake structure

Given the reference inflow wind speed obtained by the Diamond Scan, wake deficit profiles can be calculated in the measurement plane. These are based on horizontal wind speed retrievals from the dual-Doppler measurements. Deficit profiles are calculated at 1, 2 and 3 D downstream of the wind turbine, where the velocity deficit in each point i of a profile is defined as:

$$\Delta V_i = \left(1 - \frac{V_i}{V_{\text{inflow}}}\right) \tag{2}$$

An example of a 10-minute average period from 6:49 to 6:59 UTC, 7 June 2015 is shown in figure 7a. The profile extracted at 1 D distance (figure 7b) shows a deficit with a local minimum in the wake centre, caused by a lower energy extraction around the nacelle. With increasing distance this minimum disappears and the maximum deficit is decreasing from over 70% to 50%.

The averaged wake deficit for all available 10-minute periods in sectors to towards the northeast and southwest ($54° \pm 15°$ and $234° \pm 15°$) are calculated. The average maximum deficits are 53% and 55% at 1 D downstream for the northeastern and southwestern sectors, respectively. For downstream distances of 2 D and 3 D it is noticed that in some periods the wake leaves the Diamond Scan plane in the vertical direction and thus, it is not entirely captured. Such a misalignment causes that deficits profiles measured with the Diamond scan are not necessarily located in the wake center. Nevertheless, close to the turbine, the wake misalignment with the Diamond Scan is expected to be small, which allowed calculating an average deficit for specific sectors in a distance of one rotor diameter. Consequently, only selected periods can be investigated over the entire length of the Diamond Scan.

4.2 Wake Propagation

The wind turbine wake propagation is investigated for wind directions in a $30°$ sector centred around the wind turbine transect ($54°$). This sector is covered by both the Diamond Scan and the Transect Scan which makes a combined use of the scans possible. Moreover, this transect is aligned with the centre of the SR Wake Scan. The investigation of 10-minute averaged scans reveals significant vertical displacements of the wake. Considering both the state of the atmosphere captured by the Transect Scan and the WRF simulation results, four different cases are identified (see table 1).

Examples for each case are presented in figure 9. The first two cases are observed between sunset and sunrise during stable atmospheric conditions. These periods are categorised by distinct atmospheric layers of different wind speeds and directions. The Transect Scans for some nocturnal periods show a gravity wave pattern which interacts with the wake, displacing it downwards (case 1) in the direction of the leeward ridge slope, causing strong displacements of the wake centre. The wake leaves the plane of the Diamond Scan after one or two rotor diameters downstream and continuous to propagates above the plane of the Transect Scan.
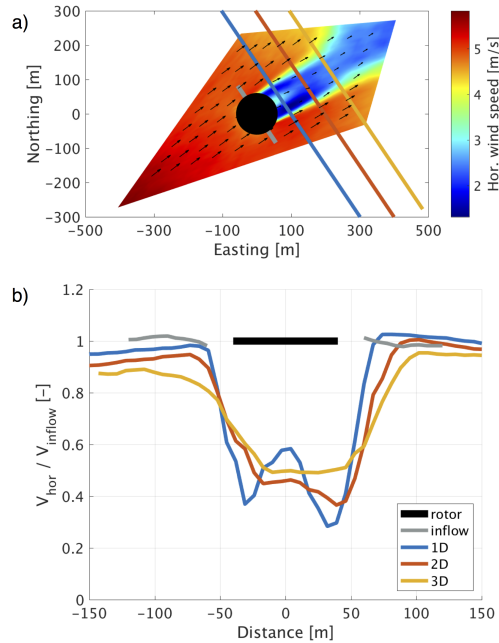
Figure 7. Wind turbine wake deficit observed with the Diamond Scan (10-minute averaged period measured on June 7, 2015 from 06:~~49~~18 to 06:~~59~~28): a) Diamond Scan with lines indication the position of deficit profiles; b) wake deficit profiles. The average tip speed ratio during this period is $\lambda = 6.7$ and the power coefficient is $c_p = 1.7 \cdot 10^{-4}$.

Table 1. Wake categorisation according to stratification (the stratification is defined by the Obukhov length: stable $1/L_{mo} > 0.01$, neutral $0.01 > 1/L_{mo} > -0.01$, unstable $1/L_{mo} < -0.01$). Periods with gravity waves are identified by visual inspection of the Transect scans.

Case	Stratification	Wake advection
1	stable + gravity wave	downwards
2	stable	straight
3	neutral	straight
4	unstable	upwards

To relate the wake shapes in the Diamond Scan to a wake displacement, the cross-sectional area of an idealised wake and the Diamond Scan plane is geometrically modelled. The model, which contains code originally presented by Calinon (2009), represents the wake by a cone with an off-axis opening angle of $\Theta = 10°$ corresponding to the wake expansion determined at 2D distance for the period depicted in figure 9 (case 2). By varying the vertical angle of the cone, the length of the cross-section visible in the Diamond Scan is derived. The model shows that wakes are staying within the dimensions of the Diamond Scan plane for vertical displacement angles from $10°$ to ~~-19~~$-19°$, see figure 8. For larger displacements only a cross-section of wakes is visible.
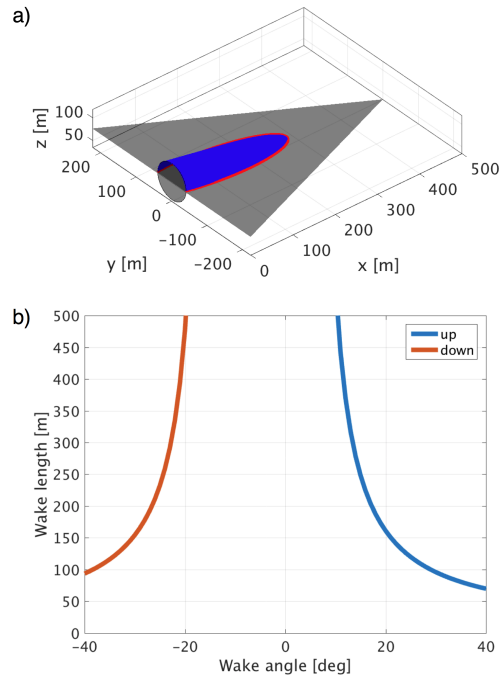
Figure 8. Wake cross section model: a) Model schematic for a negative vertical wake angle of -23° (black plane: one half of the Diamond Scan plane, blue plane: cone section representing the wake, red line: cross section, black circle: rotor plane); b) Derived length of the wake cross section in the Diamond Scan for different wake angles with a wake expansion angle of $\Theta = 10°$. The asymmetry of the model results from the negatively inclined scanning plane.

The categorisation and the geometrical model is applied to all periods for which the Transect Scan and the Diamond Scan are available and the wind direction falls in the relevant sector. The wake length is determined from contour plots of the Diamond scan and Transect scan determines the direction of vertical displacement. In total 21 periods are categorised in an upwards, downwards or straight wake propagation in relation to the atmospheric stability, see figure 10a. ~~The atmospheric stability is~~

5 ~~expressed by one over the Obukhov length, where values greater than zero (> 0.01) are indicating a stable atmosphere, values close to zero neutral conditions and values smaller than zero (< −0.01) unstable conditions.~~ Two of the 21 periods ~~are showing~~ show a wake centre displaced downwards, six a straight propagation of the wake and the remaining fourteen periods show an upwards moved wake centre. The wake propagates straight or downwards depending on the presence of a gravity wave during stable conditions. Displacements upwards are observed mainly during unstable conditions. Inconsistencies of the categorisation

10 and calculated stability occur in the evening times at around 18:00, where displacements downwards are observed and the WRF simulation shows neutral conditions. A reason for this can be that the WRF simulation has problems resolving the exact time of the transition from unstable to neutral conditions. For a clarification~~of this~~, direct measurements of the stability are necessary. However, the simulations agrees in general with the categorisation and show an expected diurnal cycle for the period of the

campaign. Neutral conditions are expected at the transition from stable to unstable periods (or vice versa). The cross-sectional model shows wake angles from 21° to 29° during stable conditions and angles of up to ~~28~~ 28° in combination with the presence of an internal wave (~~figure~~ Figure 10b).

Results of the of the short-range WindScanner scan in one rotor diameter distance indicate an equal behaviour of the wake propagation. Periods are observed where the wake centre is moved downwards or lifted upwards. In case of a downwards moved wake it is observed that there is no clear distinction between the wake and the flow field under the rotor ~~, see figure~~ (Figure 11 b). The upwards moved case ~~one~~ on the other hand shows clearly the flow passing between ground and rotor disc. The short-range could provide only a small amount of measurements, due to a small scanning plan, which only allowed to capture the wake for a narrow sector of wind directions and technical problems with the system.

5 Summary and conclusions

Measurement data from six scanning lidars have been analysed with the purpose of describing the wind turbine wake propagation in complex terrain. The data, recorded in the summer of 2015, was collected at a site with highly complex orography in the centre of Portugal, near the town of Perdigão. The analysis focuses on the vertical wake propagation under different atmospheric stability conditions, whose influence is generally ignored in computational flow simulations, namely those performed for wind-farm layout-design. The combined analysis of a horizontal scanning plane, centred around the wind turbine, and a transect scan of radial wind speeds in that sector revealed strong vertical wake angles. In total four different wake cases are identified that show, among horizontal wake propagation, strong displacements upwards and downwards of the wake during stable and unstable atmospheric conditions. These displacements are caused by the flow field that is influenced by the atmospheric stability and the orographic structure of the terrain around the turbine. By including data from a WRF simulation ~~providing~~ that provides estimates of the atmospheric stability in terms of the Obukhov length, a correlation between wake angles and stability is identified. During unstable conditions, the wake is lifted up by up to 29°. During stably-stratified conditions the wake deflection is dependent on the occurrence of gravity waves as these force the wake to follow the terrain, resulting in downward wake angles reaching ~~28~~ 28°. Under neutral conditions the wake propagates approximately horizontally despite of the complex orography. Wake deficits of 70% are measured in 1 D distance, decreasing to 50% in ~~3D~~ 3 D distance.

This study shows that the wake propagation is highly complex and strongly depended on the stability conditions and the terrain orography. The question "Does the wake follow the terrain?" is answered: In some cases it does, but in the majority of situation observed in this investigation the wake ~~is not following~~ does not follow the terrain. However, the wake could not be observed over the full vertical range with the scanning trajectories of this campaign as the designed trajectories were addressing several scientific objectives at the same time (see Vasiljević et al., 2017). For future investigations of the wind turbine wake propagation in complex terrain, it can be recommended to design scanning trajectories in a way that they cover a wider vertical range and to focus optimally only on a single scientific objective. Furthermore, a nacelle mounted spinner lidar (Mikkelsen et al., 2010) could provide more detailed information about the inflow to the turbine, as this investigation showed that it is challenging to describe the inflow in complex terrain.
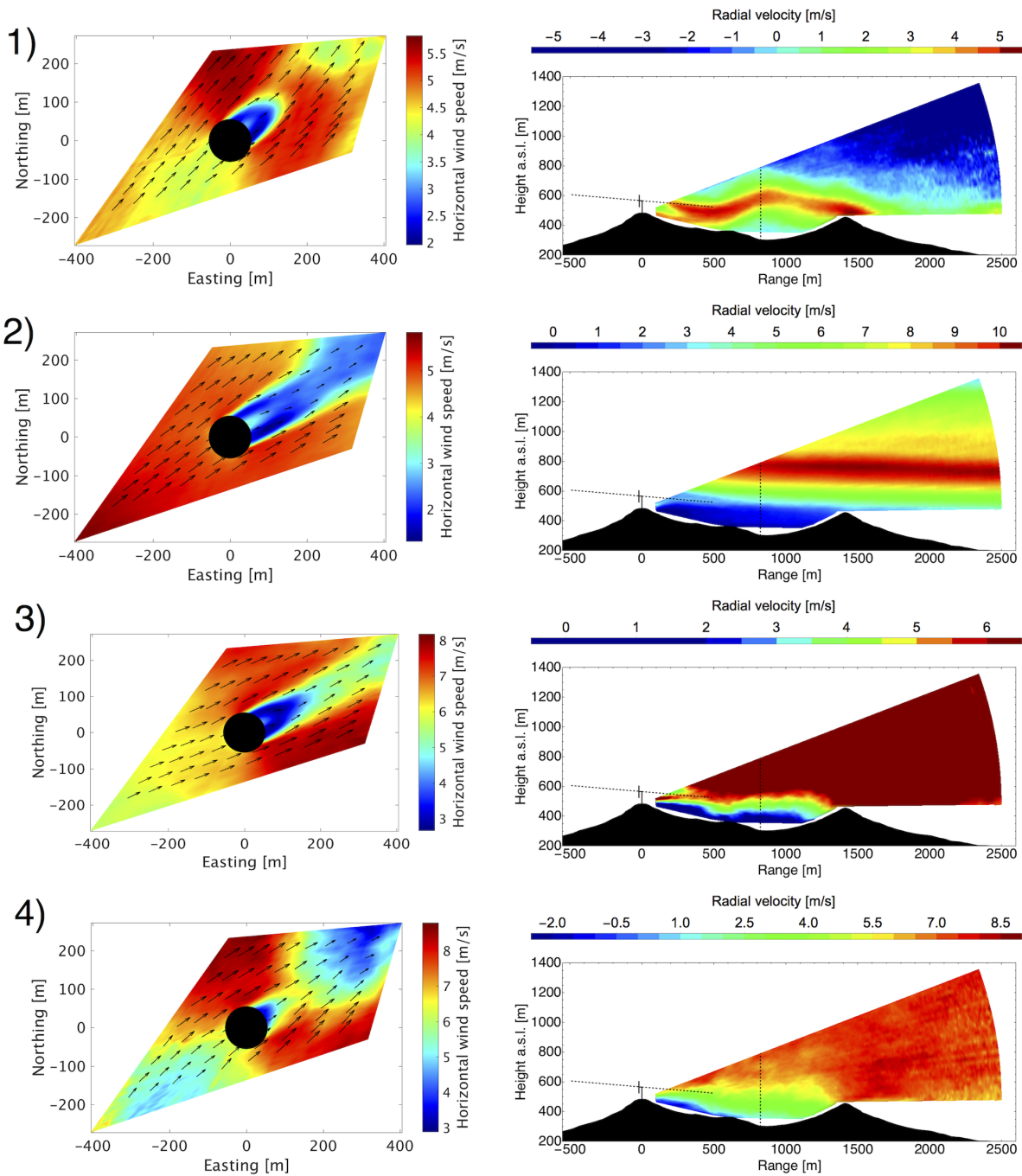
Figure 9. Observed wake cases with the Diamond Scan (left) and Transect Scan (right). 1) downwards displaced wake, stable atmospheric conditions + gravity wave, 2) no displacement, stable atmos. conditions, 3) no displacement, neutral atmos. conditions 4) upwards displaced wake, unstable atmos. conditions. (measurements of example periods taken: 1) ~~June 9 2015~~ 02:52 ~~to ~~ 03:02 UTC 9 June 2015, 2) ~~June 7 2015~~ 06:18 ~~to ~~ 06:28 UTC 7 June 2015, 3) ~~June 10 2015~~ 22:20 ~~to ~~ 22:30 UTC 10 June 2015, 4) ~~June 10 2015~~ 11:16 ~~to ~~ 11:26 UTC 10 June 2015)
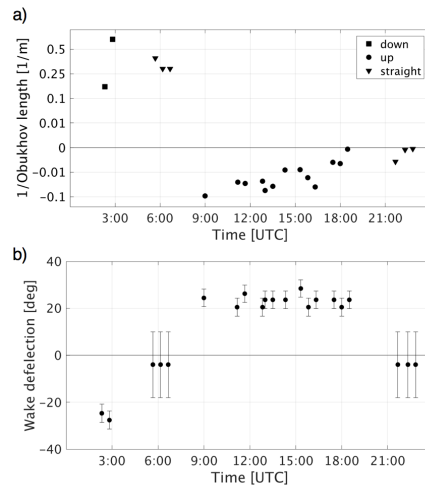
Figure 10. ~~Diurnal cycle of observed wake~~ Wake displacements as a function of the time of the day: a) direction of displacement relative to one over the Obukhov length; b) wake deflection angles according to the cross sectional model. The error is indicating the sensitivity to the wake expansion angle for changes of $\Delta\Theta=\pm2°$ and for periods with a straight propagation the range in which wakes are fully covered by the Diamond Scan.
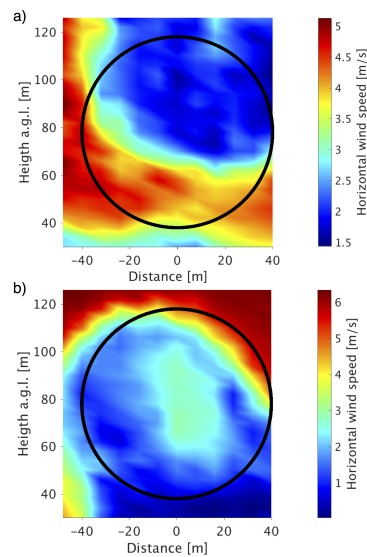
Figure 11. Short-range WindScanner wake measurements a) upwards moved wake (10-minute period ~~of May 11, 2015~~ from 19:20 ~~to~~ – 19:30 UTC 11 May 2015) and b) downwards moved wake (10-minute period ~~of May 12, 2015 from~~ form 00:50 ~~to~~ – 01:00 UTC 12 May 2015), further examples are presented in Hansen et al. (2016). Black circle: projected rotor disc.

References

Abkar, M. and Porté-Agel, F.: Influence of atmospheric stability on wind-turbine wakes: A large-eddy simulation study, Physics of Fluids, 27, 035 104, 2015.

Aitken, M. L. and Lundquist, J. K.: Utility-scale wind turbine wake characterization using nacelle-based long-range scanning lidar, Journal of Atmospheric and Oceanic Technology, 31, 1529–1539, 2014.

Aitken, M. L., Kosović, B., Mirocha, J. D., and Lundquist, J. K.: Large eddy simulation of wind turbine wake dynamics in the stable boundary layer using the Weather Research and Forecasting Model, Journal of Renewable and Sustainable Energy, 6, 033 137, 2014.

Barthelmie, R. J., Frandsen, S. T., Nielsen, M., Pryor, S., Rethore, P.-E., and Jørgensen, H. E.: Modelling and measurements of power losses and turbulence intensity in wind turbine wakes at Middelgrunden offshore wind farm, Wind Energy, 10, 517–528, 2007.

Bhaganagar, K. and Debnath, M.: The effects of mean atmospheric forcings of the stable atmospheric boundary layer on wind turbine wake, Journal of Renewable and Sustainable Energy, 7, 013 124, 2015.

Bingöl, F., Trujillo, J. J., Mann, J., and Larsen, G. C.: Fast wake measurements with LiDAR at Risø test field, in: IOP Conference Series: Earth and Environmental Science, vol. 1, IOP Publishing, 2008.

Bingöl, F., Mann, J., and Larsen, G. C.: Light detection and ranging measurements of wake dynamics part I: one-dimensional scanning, Wind energy, 13, 51–61, 2010.

Bodini, N., Zardi, D., and Lundquist, J. K.: Three-dimensional structure of wind turbine wakes as measured by scanning lidar, Atmospheric Measurement Techniques, 10, 2881, 2017.

Bustamante, A., Vera-Tudela, L., and Kühn, M.: Evaluation of wind farm effects on fatigue loads of an individual wind turbine at the EnBW Baltic 1 offshore wind farm, in: Journal of Physics: Conference Series, vol. 625, p. 012020, IOP Publishing, 2015.

Calinon, S.: Robot Programming by Demonstration: A Probabilistic Approach, EPFL/CRC Press, ePFL Press ISBN 978-2-940222-31-5, CRC Press ISBN 978-1-4398-0867-2, 2009.

CLC: CORINE Land Cover 100 m raster data, European Environmental Agency (EEA), http://www.eea.europa.eu/ds_resolveuid/a47ee0d3248146908f72a8fde9939d9d, 2006.

Conway, J. T.: Analytical solutions for the actuator disk with variable radial distribution of load, Journal of Fluid Mechanics, 297, 327–355, 1995.

Dee, D. P., Uppala, S., Simmons, A., Berrisford, P., Poli, P., Kobayashi, S., Andrae, U., Balmaseda, M., Balsamo, G., Bauer, P., et al.: The ERA-Interim reanalysis: Configuration and performance of the data assimilation system, Quarterly Journal of the royal meteorological society, 137, 553–597, 2011.

Englberger, A. and Dörnbrack, A.: Impact of the Diurnal Cycle of the Atmospheric Boundary Layer on Wind-Turbine Wakes: A Numerical Modelling Study, Boundary-Layer Meteorology, pp. 1–26, 2017.

Hahmann, A., Witha, B., Rife, D., Frouzakis, N., Junk, C., Sile, T., Baltscheffsky, M., Dörenkämper, M., Ezber, Y., Gonzalez-Rouco, F., Mentes, S., Navarro, J., Söderberg, S., and Unal, Y.: Description of the Probabilistic Wind Atlas Methodology, Deliverable D3.1, NEWA - New European Wind Atlas, 2017.

Hahmann, A. N., Vincent, C. L., Peña, A., Lange, J., and Hasager, C. B.: Wind climate estimation using WRF model output: Method and model sensitivities over the sea, International Journal of Climatology, 35, 3422–3439, 2015.

Hansen, K., Larsen, G., Menke, R., Vasiljević, N., Angelou, N., Feng, J., Zhu, W., Vignaroli, A., W, W. L., Xu, C., and Shen, W.: Wind turbine wake measurement in complex terrain, Journal of Physics: Conference Series, 753, 032 013, 2016.

Hansen, M. O.: Aerodynamics of wind turbines, Routledge, 2015.

Herges, T., Maniaci, D., Naughton, B., Mikkelsen, T., and Sjöholm, M.: High resolution wind turbine wake measurements with a scanning lidar, in: EWEA Wake Conference, To Be Published, 2017.

IEC: IEC 61400-12-1 - Part 12-1: Power performance measurements of electricity producing wind turbines, Tech. rep., International Electrotechnical Commission, 2005.

Iungo, G. and Porté-Agel, F.: Measurement procedures for characterization of wind turbine wakes with scanning Doppler wind LiDARs, Advances in Science and Research, 10, 71–75, 2013.

Käsler, Y., Rahm, S., Simmet, R., and Kühn, M.: Wake measurements of a multi-MW wind turbine with coherent long-range pulsed Doppler wind lidar, Journal of Atmospheric and Oceanic Technology, 27, 1529–1532, 2010.

Krishnamurthy, R., Choukulkar, A., Calhoun, R., Fine, J., Oliver, A., and Barr, K.: Coherent Doppler lidar for wind farm characterization, Wind Energy, 16, 189–206, 2013.

Machefaux, E., Larsen, G. C., Troldborg, N., Hansen, K., Angelou, N., Mikkelsen, T., Mann, J., et al.: Investigation of wake interaction using full-scale lidar measurements and large eddy simulation, Wind Energy, 19, 1535–1551, 2016.

Mann, J., Angelou, N., Arnqvist, J., Callies, D., Cantero, E., Arroyo, R. C., Courtney, M., Cuxart, J., Dellwik, E., Gottschall, J., et al.: Complex terrain experiments in the New European Wind Atlas, Phil. Trans. R. Soc. A, 375, 20160 101, 2017.

Mikkelsen, T., Mann, J., Courtney, M., and Sjöholm, M.: Windscanner: 3-d wind and turbulence measurements from three steerable Doppler lidars, in: IOP conference series: earth and environmental science, vol. 1, p. 012018, IOP Publishing, 2008.

Mikkelsen, T., Hansen, K. H., Angelou, N., Sjöholm, M., Harris, M., Hadley, P., Scullion, R., Ellis, G., and Vives, G.: Lidar wind speed measurements from a rotating spinner, in: 2010 European Wind Energy Conference and Exhibition, 2010.

Mirocha, J., Kosovic, B., Aitken, M., and Lundquist, J.: Implementation of a generalized actuator disk wind turbine model into the weather research and forecasting model for large-eddy simulation applications, Journal of Renewable and Sustainable Energy, 6, 013 104, 2014.

Mirocha, J. D., Rajewski, D. A., Marjanovic, N., Lundquist, J. K., Kosović, B., Draxl, C., and Churchfield, M. J.: Investigating wind turbine impacts on near-wake flow using profiling lidar data and large-eddy simulations with an actuator disk model, Journal of Renewable and Sustainable Energy, 7, 043 143, 2015.

Peña, A. and Hahmann, A. N.: Atmospheric stability and turbulence fluxes at Horns Rev—an intercomparison of sonic, bulk and WRF model data, Wind Energy, 15, 717–731, 2012.

Rhodes, M. E. and Lundquist, J. K.: The effect of wind-turbine wakes on summertime US midwest atmospheric wind profiles as observed with ground-based Doppler lidar, Boundary-layer meteorology, 149, 85–103, 2013.

Skamarock, W. C., Klemp, J. B., Dudhia, J., Gill, D. O., Barker, D. M., Duda, M. G., Huang, X.-Y., Wang, W., and Powers, J. G.: A Description of the Advanced Research WRF Version 3, Technical Note NCAR/TN-475+STR, National Center for Atmospheric Research, Boulder CO USA, 113 pp., 2008.

Smalikho, I., Banakh, V., Pichugina, Y., Brewer, W., Banta, R., Lundquist, J., and Kelley, N.: Lidar investigation of atmosphere effect on a wind turbine wake, Journal of Atmospheric and Oceanic Technology, 30, 2554–2570, 2013.

Thomsen, K. and Sørensen, P.: Fatigue loads for wind turbines operating in wakes, Journal of Wind Engineering and Industrial Aerodynamics, 80, 121–136, 1999.

Troen, I. and Petersen, E. L.: European Wind Atlas, Risø National Laboratory, 1989.

Trujillo, J.-J., Bingöl, F., Larsen, G. C., Mann, J., and Kühn, M.: Light detection and ranging measurements of wake dynamics. Part II: two-dimensional scanning, Wind Energy, 14, 61–75, 2011.

Vasiljevic, N.: A time-space synchronization of coherent Doppler scanning lidars for 3D measurements of wind fields, Ph.D. thesis, Technical University of Denmark, Department of Wind Energy, 2014.

Vasiljević, N., Lea, G., Courtney, M., Cariou, J.-P., Mann, J., and Mikkelsen, T.: Long-range WindScanner system, Remote Sensing, 8, 896, 2016.

5 Vasiljević, N., Palma, J. M., Angelou, N., Matos, J. C., Menke, R., Lea, G., Mann, J., Courtney, M., Ribeiro, L. F., and Gomes, V. M.: Perdigão 2015: methodology for atmospheric multi-Doppler lidar experiments, Atmospheric Measurement Techniques, 10, 3463, 2017.

Vollmer, L., van Dooren, M., Trabucchi, D., Schneemann, J., Steinfeld, G., Witha, B., Trujillo, J., and Kühn, M.: First comparison of LES of an offshore wind turbine wake with dual-Doppler lidar measurements in a German offshore wind farm, in: Journal of Physics: Conference Series, vol. 625, IOP Publishing, 2015.

10 Vollmer, L., Steinfeld, G., Heinemann, D., and Kühn, M.: Estimating the wake deflection downstream of a wind turbine in different atmospheric stabilities: an LES study, Wind Energy Science, 1, 129–141, 2016.

Wagner, R., Courtney, M., Gottschall, J., and Lindelöw-Marsden, P.: Accounting for the speed shear in wind turbine power performance measurement, Wind Energy, 14, 993–1004, 2011.

Witze, A.: World's largest wind-mapping project spins up in Portugal., Nature, 542, 282, 2017.